

# Instability of dilute granular flows on rough slope

Namiko MITARAI\* and Hiizu NAKANISHI\*\*

*Department of Physics, Kyushu University 33, Fukuoka 812-8581*

(Received October 24, 2018)

We study numerically the stability of granular flow on a rough slope in collisional flow regime in the two-dimension. We examine the density dependence of the flowing behavior in low density region, and demonstrate that the particle collisions stabilize the flow above a certain density in the parameter region where a single particle shows an accelerated behavior. Within this parameter regime, however, the uniform flow is only metastable and is shown to be unstable against clustering when the particle density is not high enough.

**KEYWORDS:** granular flow, surface flow, clustering, inelastic collision, simulation, discrete element method

Granular flow on a slope is one of the simplest situations to see the characteristic behavior of granular dynamics. When the inclination angle is smaller than a certain value (the angle of repose), the material never flows because of the stress sustained by the friction. Beyond that angle, the surface layers of the material may flow like a fluid, but the bottom part of the materials may remain solidified when the inclination angle is not steep enough.<sup>1)</sup> If the inclination is increased further, all of the material starts to flow rapidly, and the interaction between particles or between a particle and the slope is dominated by the inelastic collision, rather than friction.

Many researches have been done in such a collisional flow regime, but most of them focus on the property of the uniform flow.<sup>2,3,4)</sup> In such researches, the depth dependence of the flow properties such as velocity or density profile is investigated, assuming that the flow is uniform in the direction along the slope. It is known, however, that the granular materials have the tendency to cluster due to the inelastic collision, which causes the formation of density waves in the case of granular flow in a vertical pipe.<sup>6,5)</sup> Therefore, it is natural to expect that this tendency will cause some instability in the uniform flow on a slope.

Granular flow of an independent particle, or a single particle behavior, has been studied, and has been found to show three types of motion depending on the inclination angle and roughness of the slope.<sup>7,8,9)</sup> For the fixed roughness of the slope, the following behaviors are observed upon increasing the inclination angle: (i)The particle stops after a few collisions with the slope for any initial velocity (regime A). (ii)The particle quickly reaches a constant averaged velocity in the direction along the slope and shows almost steady motion; the averaged velocity does not depend on the initial condition (regime B). (iii)The particle jumps and accelerates as it goes down the slope (regime C).

In the present work, we study how the above single particle picture is modified in the collisional flow with

finite density by the particle collisions. Based on numerical simulations, we determine the parameter region where the uniform collisional flow is realized with the finite density, and examine the stability of the uniform flow.

We employed the discrete element method<sup>10,11)</sup> with the normal and the tangential elastic force and dissipation. In the simulations, granular particles are modeled by two-dimensional disks with mass  $m$  and diameter  $d$ . When the two disks  $i$  and  $j$  at positions  $\mathbf{r}_i$  and  $\mathbf{r}_j$  with velocities  $\mathbf{v}_i$  and  $\mathbf{v}_j$  and angular velocities  $\omega_i$  and  $\omega_j$  are in contact, the force acting on the particle  $i$  from the particle  $j$  is calculated as follows: The normal velocity  $v_n$  and the tangential velocity  $v_t$  are given by

$$v_n = \mathbf{v}_{ij} \cdot \mathbf{n}, \quad v_t = \mathbf{v}_{ij} \cdot \mathbf{t} - (d/2)(\omega_i + \omega_j), \quad (1)$$

with the normal vector  $\mathbf{n} = \mathbf{r}_{ij}/|\mathbf{r}_{ij}| = (n_x, n_y)$  and the tangential vector  $\mathbf{t} = (-n_y, n_x)$ . Here,  $\mathbf{r}_{ij} = \mathbf{r}_j - \mathbf{r}_i$  and  $\mathbf{v}_{ij} = \mathbf{v}_j - \mathbf{v}_i$ . Then the normal force  $F_{ij}^n$  and the tangential force  $F_{ij}^t$  acting on the particle  $i$  from the particle  $j$  are given by

$$F_{ij}^n = -k_n(d - |\mathbf{r}_{ij}|) + \eta_n v_n, \quad (2)$$

$$F_{ij}^t = \min(|h_t|, \mu |F_{ij}^n|) \text{sign}(h_t), \quad (3)$$

with

$$h_t = k_t u_t + \eta_t v_t, \quad u_t = \int_{t_0}^t v_t dt. \quad (4)$$

Here,  $u_t$  is the tangential displacement, and  $t_0$  is the time when the particles started to contact.  $k_n$  and  $k_t$  are elastic constants,  $\eta_n$  and  $\eta_t$  are damping parameters, and  $\mu$  is the Coulomb friction coefficient for sliding friction. Each particle is also subject to the gravity, and the gravitational acceleration is given by  $\mathbf{g} = g(\sin \theta, -\cos \theta)$ . The surface of the slope is made rough by gluing the particles identical with the moving ones with spacing  $2\epsilon d$  with  $\epsilon = 0.001$  (Fig. 1). The periodic boundary condition is imposed in the  $x$  direction. The system size  $L$  is determined by the number of the particles glued on the slope  $n_s$  as  $L = (1 + 2\epsilon)d n_s$ .

All quantities which appear in the following are given

\* E-mail: namiko@stat.phys.kyushu-u.ac.jp

\*\* E-mail: naka4scp@mbox.nc.kyushu-u.ac.jp

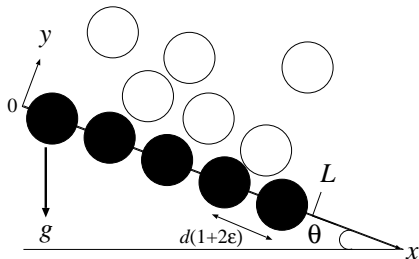


Fig. 1. A schematic illustration of the system geometry.

Table I. Parameters used in the simulations.

$k_n$	$k_t$	$\eta_n$	$\eta_t$	$\mu$
$5 \times 10^4$	$(5 \times 10^4)/3$	35.68	$35.68/3$	0.5

in the non-dimensionalized form in terms of the length unit  $d$ , the mass unit  $m$ , and the time unit  $\tau = (d/g)^{1/2}$ . The parameters used in the simulations are tabulated in Table I. With these parameters, the normal restitution coefficient (the ratio of normal relative velocities of pre- and post-collision)  $e_n$  turns out to be around 0.7. We integrated the equations of motions using the predictor-corrector method in the third order with a constant time step  $\delta t = 1 \times 10^{-4}$ .

We first investigate how the uniform collisional flow appears when we increase the density of flowing particles from the one particle limit.

As we have referred, a particle on a slope shows three types of behavior depending on the value of  $\theta$ . It is known, however, that the boundary between the regime B (the constant velocity regime) and C (the acceleration regime) is not sharp; there is a parameter region where the particle can attain steady state or can accelerate, depending on the initial condition. We should also note that, when the initial kinetic energy of the particle is too small, the particle may stop in the regime B and in part of the regime C. In the present model with the parameters in Table I, it turns out that the regime A roughly corresponds to the region  $\sin \theta \lesssim 0.11$ , the regime B to  $0.11 \lesssim \sin \theta \lesssim 0.14$ , and the regime C to  $0.16 \lesssim \sin \theta$ .

Now we focus on what happens when the number of moving particles  $n$  is increased with the finite  $L$ . It is easy to expect that the dissipation becomes larger upon increasing  $n$ , because the collisions between particles or a particle and the slope become more frequent. Therefore it is obvious that all the particles will stop irrespective of the initial condition if  $\theta$  is in the regime A. Even for any  $\theta$  within the regime B, it turns out that the collisions between particles eventually stop all the particles.

We examine closely the flowing behavior for the larger inclination angle  $\theta$  in the regime C. The situation is presented by showing the simulations with  $\sin \theta = 0.45$  and  $L = 20.04$ . We set the initial condition as follows:

$$x_i(0) = (L/n)(i-1), \quad y_i(0) = (1+2\epsilon)d + \alpha\xi_i, \quad (5)$$

$$u_i(0) = 0, \quad v_i(0) = 0, \quad \omega_i(0) = 0, \quad (6)$$

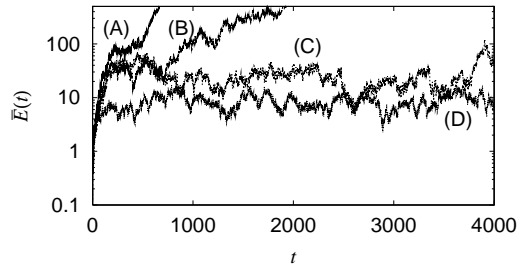


Fig. 2. The semi-log plot of  $\bar{E}(t)$  for (A) $\rho = 0.50$ , (B) $\rho = 0.60$ , (C) $\rho = 0.65$ , and (D) $\rho = 1.00$ , with  $\sin \theta = 0.45$  and  $L = 20.04$ .  $\bar{E}(t)$  continues to grow when  $\rho \leq 0.60$ , while it is bounded when  $\rho \geq 0.65$ .

where  $x_i(t)$  ( $y_i(t)$ ) and  $u_i(t)$  ( $v_i(t)$ ) are the coordinate and the velocity of center of mass of the  $i$ th particle at time  $t$  in the  $x$  ( $y$ ) direction, respectively.  $\xi_i$  is a random number uniformly distributed over the interval  $[0, 1]$ . The appropriate value of  $\alpha$  is a few times the diameter, and we adopted  $\alpha = 3 \sim 4$  in actual simulations. In the following, we define the 'density' of the particles as  $\rho = n/L$ . In the simulations with  $L = 20.04$ , we do not observe non-uniformity along the slope in the particle distribution, therefore the parameter  $\rho$  is enough to describe the situation. In order to characterize the qualitative difference of accelerated behavior in the regime C and the uniform flow, we investigate the  $\rho$  dependence of the averaged kinetic energy  $\bar{E}(t)$  defined as

$$\bar{E}(t) = \frac{1}{n} \sum_{i=1}^n E_i(t), \quad (7)$$

where  $E_i(t)$  is the kinetic energy of the  $i$ th particle at time  $t$ ;

$$E_i(t) = \frac{1}{2}m [u_i(t)^2 + v_i(t)^2] + \frac{1}{2}I\omega_i(t)^2, \quad (8)$$

with  $I = md^2/8$ .

In Fig. 2, the time evolutions of  $\bar{E}(t)$  are shown for several values of  $\rho$ . When  $\rho$  is small ( $\rho \leq 0.60$ ),  $\bar{E}(t)$  grows rapidly and continuously, but the growth rate become smaller as  $\rho$  increases. In this region, each particle jumps and rarely collides with each other. When  $\rho \geq 0.65$ ,  $\bar{E}(t)$  still grows rapidly in early stage, but its long-time behavior seems to be bounded and fluctuate around a constant value. In this case each particle also jumps, but often collides with other particles and is prevented from jumping up infinitely. Based on this observation, we define the uniform flow in the low-density limit as the flow which is uniform along the flow direction with the value of  $\bar{E}(t)$  being bounded, namely the energy dissipation due to inelastic collisions balances with the energy gain from the gravity.

The average value of the kinetic energy  $\bar{E}$  in the uniform flow should be related to  $X$ , the distance between collisions along the slope, by  $(1 - e_n^2)\bar{E} \sim mgX \sin \theta$ , because the energy gain by the gravitation should balance with the loss due to inelastic collisions. The simulation shows the typical value of  $X$  to be  $O(1) \sim O(10)$  in the uniform flow, thus we expect  $\bar{E}$  to be  $O(1) \sim O(10)$ . On

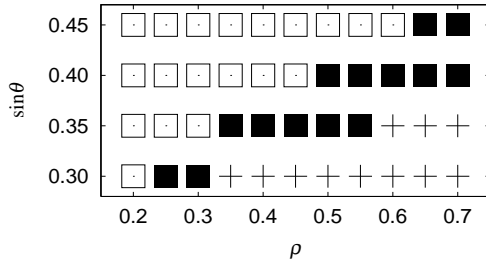


Fig. 3. The ‘phase diagram’ obtained from the simulations with  $L = 20.04$ . The accelerated regime (open box), the uniform flow regime (filled box), and the regime where all the particles stop (plus) are shown when more than 50 % of trials result in the corresponding behavior.

the other hand,  $\bar{E}$  diverges in the accelerated regime.

Figure 3 shows the ‘phase diagram’ summarizing the behavior in terms of  $\theta$  and  $\rho$  obtained from numerical simulations. In order to obtain the diagram, 10 simulations with  $L = 20.04$  were done for each  $\theta$  and  $\rho$ . We identify the three behaviors, namely (i) accelerated motion, (ii) uniform flow, and (iii) static state where all the particles come to rest, by the following criterion; the system is determined to be in the accelerated motion (in the static state) if  $\bar{E}(t)$  exceeds 500 (becomes zero) by  $t = 20,000$ . It is determined to be the uniform flow if neither of them happen. The final behavior sometimes depends on the initial condition. This, we believe, is due to the finite size effect. Each point in Fig. 3 is determined to be in one of these regimes if more than 50 % of the trials show the one of the above behaviors. It is expected that, if we could take the  $L \rightarrow \infty$  limit with fixed  $\rho$  with keeping the particle distribution uniform along the slope, such initial condition dependence should disappear.

Now we examine the stability of the uniform flow by taking the system size large enough to observe non-uniformity along the slope. First we show the simulation results of the flow in the system with  $\sin\theta = 0.45$ ,  $L = 1002$  and  $n = 1000$ , i.e.  $\rho = 1.0$ . The initial condition is also given by eq. (6), therefore the particles are uniformly distributed along the slope at first. Figure 4 shows the time evolution of the flux  $\Phi(t)$  defined as the number of the particles which pass  $x = L/2$  during the time interval  $\Delta t = 10$ . After a short transient time, the flux becomes almost constant with small fluctuations ( $300 \lesssim t \lesssim 2000$ ), which indicates uniform flow is realized. Then  $\Phi(t)$  shows large fluctuation which grows in the course of time ( $2000 \lesssim t \lesssim 3000$ ); this means the clustering behavior is triggered by the fluctuation. Finally  $\Phi(t)$  begins to oscillate almost periodically with large amplitude ( $t \gtrsim 3000$ ). This oscillation of the flux indicates that one large cluster of particles travels in the system with almost constant velocity; we can see that the cluster is stable once it is formed. From this observation, we expect that the uniform flow is not stable against clustering. Considering the fact that the uniform flow has a finite life time during which the flow seems fairly stable, we expect that a fluctuation of finite size is necessary to

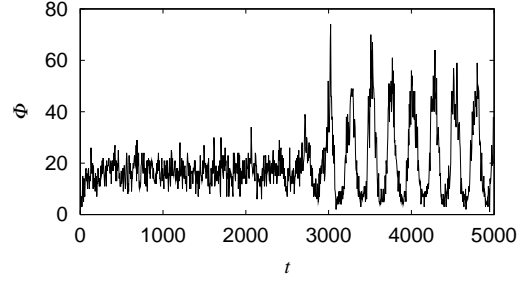


Fig. 4. The time evolution of the flux  $\Phi(t)$  in the simulation with  $L = 1002$  and  $\rho = 1.0$ . A fluctuation grows to form a cluster spontaneously.

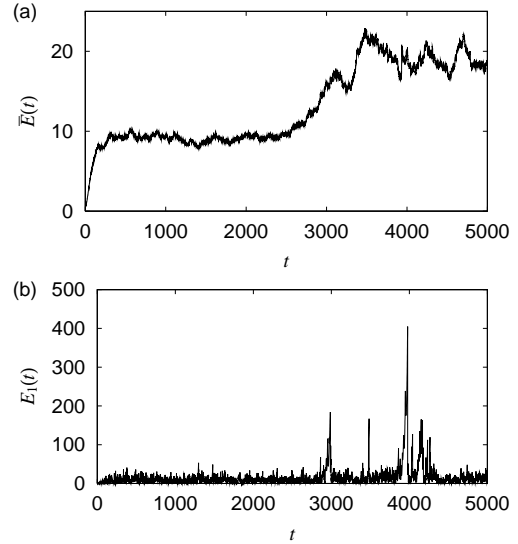


Fig. 5. The time evolution of (a)  $\bar{E}(t)$  and (b)  $E_1(t)$  in the simulation with  $L = 1002$  and  $\rho = 1.0$ . Compared with Fig. 4, we can see that, after the clustering occurs ( $t \gtrsim 3000$ ), the time averaged value of  $\bar{E}(t)$  becomes larger than that in the uniform flow stage, and  $E_1(t)$  begins to show large fluctuation.

trigger the clustering, which means the uniform flow is metastable.

In Figs. 5, the time evolutions of (a) the averaged kinetic energy  $\bar{E}(t)$  and (b) the kinetic energy of a particular particle  $E_1(t)$  are also shown. Both of them are almost constant in the stage of the uniform flow. Then  $\bar{E}(t)$  increases in  $2000 \lesssim t \lesssim 3000$ . In  $t \gtrsim 3000$ , the fluctuation of  $E_1(t)$  becomes considerably large, and  $\bar{E}(t)$  begins to fluctuate around another constant value which is larger than the one in the stage of the uniform flow. The reason why the kinetic energy increases when a cluster is formed can be understood as follows: When the cluster is formed, the region with the density lower than the threshold value to prevent the acceleration ( $\sim 0.65$  in the case of  $\sin\theta = 0.45$ , see Fig. 3.) appears locally, and particles in such a spatial region can be highly accelerated. However, the particle will be caught in the cluster sooner or later, and then quickly lose its kinetic energy. This mechanism maintains the moving cluster, and results in the large fluctuations in  $E_1(t)$ .

also examined the system size and the density depen-

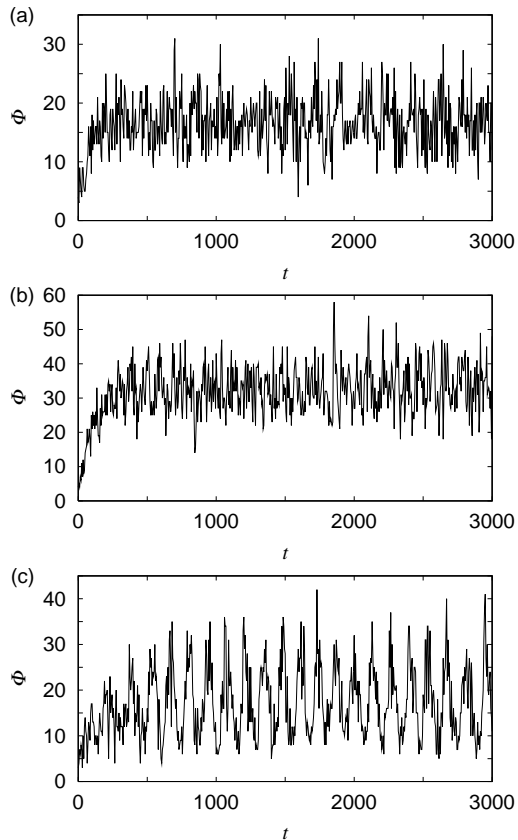


Fig. 6. The time evolution of the flux  $\Phi(t)$  in the simulation with  $L = 501$  and (a)  $\rho = 1.0$ , (b)  $\rho = 2.0$ , and (c)  $\rho = 0.75$ .

dence of the clustering. The time evolutions of the flux for a few values of densities with  $L = 501$  are also shown in Figs. 6. Figure 6 (a) shows the result with  $\rho = 1.0$  ( $n = 500$ ), which is the same density as the simulation in Fig. 4. In Fig. 6 (a), however, no clustering behavior can be seen clearly even though the fluctuation is very large. We have also simulated in the system with  $L = 250.5$  and  $\rho = 1.0$  ( $n = 250$ ), but the clustering behavior was not found, either. On the other hand, the density dependence of the system behavior can be seen in Figs. 6 (b) ( $\rho = 2.0$ ) and (c) ( $\rho = 0.75$ ). It is found that the uniform flow is maintained in Fig. 6 (b), while the clear oscillation of the flux associated with the cluster formation is seen in Fig. 6 (c). From these results, we can see the general tendency that the uniform flow tends to be stabilized as the system size is smaller or as the density is higher.

In summary, we have examined the two-dimensional granular flow on a rough slope in the collisional flow regime by numerical simulations. It was shown that the mutual collisions among particles stabilizes the flow even in the accelerated regime for a single particle system. The phase diagram was determined for the accelerated, uniform flow, and stopping regime in terms of the particle density  $\rho$  and the inclination angle  $\theta$  for a particular system size. The stability of uniform flow was also examined and we found that a large single cluster appears spontaneously out of a uniform initial state. It was shown that the smaller the particle density is, or the

larger the system size is, the less stable the uniform flow is.

Before concluding, let us make a comment on the system size dependence of the instability. Consider the situation where one large cluster, whose length along the slope is  $l$  and typical height is  $h$ , is formed. If we can neglect the particles outside the cluster, we can assume, as the first approximation, that the volume of the cluster ( $\propto lh$  for 2-dimensional case) is proportional to  $n$ . Namely we get the relation  $(l/d)(h/d) \propto n = (\rho d)(L/d)$ . Therefore, if  $(l/d)$  and  $(h/d)$  are scaled with  $(L/d)$  for fixed  $\rho$  as  $(l/d) \propto (L/d)^\beta$  and  $(h/d) \propto (L/d)^{\beta'}$ , we get the relation  $\beta' = 1 - \beta$ . Because both  $(l/d)$  and  $(h/d)$  should be increasing function of  $(L/d)$  for fixed  $\rho$ , we get an inequality for the exponent  $\beta$  that  $0 < \beta < 1$ . Then there should exist a critical system size  $L_c$  such that  $l(L_c) \sim L$ ; a cluster can exist only in the case of  $L > L_c$  for which  $l(L) < L$ , and the uniform flow become stable when  $L < L_c$ . Using similar argument, we can also predict the existence of the critical density  $\rho_c$  for a fixed  $L$ . However, we should note that the moving cluster seems to be maintained by the balance between the outgoing flux of the particles at the front of the cluster and incoming flux at the tail, therefore the motion of the particles outside the cluster may affect on the shape of the cluster in the periodic boundary condition. Therefore, the discussion here may not simply hold and the exponent  $\beta$  may depend on  $\rho$ . The scaling behaviors should be confirmed more carefully.

The spontaneous cluster formation out of uniform flow is seen also in the granular flow through a vertical pipe<sup>5,6)</sup> and in the traffic flow on a freeway.<sup>12,13)</sup> It is an interesting problem to find out whether those phenomena and the cluster formation in surface flow have a common mathematical structure at phenomenological level.

Part of the computation in this work has been done using the facilities of the Supercomputer Center, Institute for Solid State Physics, University of Tokyo.

- 
- [1] H. M. Jaeger, S. R. Nagel and R. P. Behringer: *Rev. Mod. Phys.* **68** (1996) 1259.
  - [2] T. G. Drake: *J. Fluid. Mech.* **225** (1991) 121.
  - [3] T. Pöschel: *J. Phys. II (France)* **3** (1993) 27.
  - [4] E. Azanza, F. Chevoir, and P. Moucheron: *J. Fluid. Mech.* **400** (1999) 199.
  - [5] J. Lee: *Phys. Rev. E* **49** (1994) 281.
  - [6] S. Horikawa, A. Nakahara, T. Nakayama, and M. Matsushita: *J. Phys. Soc. Jpn.* **64** (1995) 1870.
  - [7] F.-X. Riguidel, R. Jullien, G. H. Ristow, A. Hansen, and D. Bideau: *J. Phys. I (France)* **4** (1994) 261.
  - [8] G. H. Ristow, F.-X. Riguidel, and D. Bideau: *J. Phys. I (France)* **4** (1994) 1161.
  - [9] S. Dippel, G. Batrouni, and D. E. Wolf: *Phys. Rev. E* **54** (1996) 6845.
  - [10] P. A. Cundall and O. D. L. Strack: *Geotechnique* **29** (1979) 47.
  - [11] A. Shimosaka: *Funtai Simulation Nyumon* (Introduction to Simulations of Granular Materials), ed. The Society of Powder Technology, Japan (Sangyo Tosho, Tokyo, 1998) Sec. 3.2, p. 34 [in Japanese].
  - [12] D. Chowdhury, L. Santen, and A. Schadschneider: *Phys. Rep.* **329** (2000) 199.
  - [13] N. Mitarai and H. Nakanishi: *Phys. Rev. Lett.* **85** (2000) 1766.